Virology 441 (2013) 114–125

Contents lists available at SciVerse ScienceDirect

Virology

journal homepage: www.elsevier.com/locate/yviro

Mutation of the dengue virus type 2 envelope protein heparan sulfate binding sites or the domain III lateral ridge blocks replication in Vero cells prior to membrane fusion

John T. Roehrig [a,*], Siritorn Butrapet [a,1], Nathan M. Liss [a], Susan L. Bennett [b], Betty E. Luy [a], Thomas Childers [a], Karen L. Boroughs [a], Janae L. Stovall [a], Amanda E. Calvert [a], Carol D. Blair [b], Claire Y.-H. Huang [a]

[a] Division of Vector-Borne Diseases, Centers for Disease Control and Prevention, Fort Collins, CO 80521, USA
[b] Arthropod-borne and Infectious Diseases Laboratory, Department of Microbiology, Immunology, and Pathology, Colorado State University, Fort Collins, CO 80523, USA

ARTICLE INFO

Article history:
Received 11 December 2012
Returned to author for revisions
11 January 2013
Accepted 16 March 2013
Available online 6 April 2013

Keywords:
Dengue virus
Flavivirus
Envelope protein
Attachment
Heparan sulfate
Mutagenesis

ABSTRACT

Using an infectious cDNA clone we engineered seven mutations in the putative heparan sulfate- and receptor-binding motifs of the envelope protein of dengue virus serotype 2, strain 16681. Four mutant viruses, KK122/123EE, E202K, G304K, and KKK305/307/310EEE, were recovered following transfection of C6/36 cells. A fifth mutant, KK291/295EE, was recovered from C6/36 cells with a compensatory E295V mutation. All mutants grew in and mediated fusion of virus-infected C6/36 cells, but three of the mutants, KK122/123EE, E202K, G304K, did not grow in Vero cells without further modification. Two Vero cell lethal mutants, KK291/295EV and KKK307/307/310EEE, failed to replicate in DC-SIGN-transformed Raji cells and did not react with monoclonal antibodies known to block DENV attachment to Vero cells. Additionally, both mutants were unable to initiate negative-strand vRNA synthesis in Vero cells by 72 h post-infection, suggesting that the replication block occurred prior to virus-mediated membrane fusion.
Published by Elsevier Inc.

Introduction

Dengue virus (DENV), a member of *Flaviviridae* family, contains a positive-strand (+) RNA genome and three structural proteins: envelope (E), membrane (M), and capsid (C). The E protein assembles in the virion envelope as homodimer rafts, and mediates viral entry into cells via attachment, endocytosis, and fusion with endosomal membranes—delivering the capsid into the cell cytoplasm. The E protein folds into three major domains. Domain I (DI) is the central domain containing the protein "hinge" responsible for the low pH-catalyzed conformational change from homodimers to fusion-competent homotrimers. Domain II (DII) is the dimerization domain containing the fusion peptide at its tip. Domain III (DIII) is an immunoglobulin-like structure suggested to mediate binding of virus to cellular receptors (Kuhn et al., 2002; Modis et al., 2003, 2005; Mukhopadhyay et al., 2005; Nayak et al., 2009).

DENV replication begins with the attachment of virus to cellular receptors. It is now well established that cell surface glycosaminoglycans (GAGs), such as heparan sulfate (HS), can facilitate flaviviral attachment to cultured mammalian cells (Chen et al., 1997; Germi et al., 2002; Hilgard and Stockert, 2000; Hung et al., 1999). After solving the crystal structures of DENV2 and DENV3 E proteins, Modis et al. (2003, 2005) suggested that three clusters of positively charged amino acids (AAs) on E protein homodimer surface might be involved in HS binding. Cluster 1, located in DI, consists of R188, H282, K284, R286, K288, K291, and K295 (based on DENV2 E protein residue numbers) and all of these are conserved as basic residues among all 4 DENV serotypes and the Japanese encephalitis virus (JEV) complex, including West Nile virus (WNV), Murray Valley encephalitis virus (MVEV), and St. Louis encephalitis virus (SLEV). Cluster 2, located in the middle of DII near the dimer interface, includes K58, K64, K89, K122, K123, and K128 for DENV2. Unlike cluster 1, cluster 2 is less conserved among the DENV or JEV serocomplex viruses, and DENV2 contains more basic residues in this cluster than other DENV serotypes. The moderately variable cluster 3 resides (K305. K307, K310) on or near the DIII lateral ridge, including AAs important for both binding of virus-neutralizing antibody and interacting with cellular receptors (Diamond et al., 2008; Sukupolvi-Petty et al., 2007).

Because GAGs are associated with the surfaces of many cultured mammalian cells, cell-specific flaviviral attachment – if

* Corresponding author. Fax: +1 970 494 6631.
E-mail addresses: jtr1@cdc.gov, jtroehrig@hotmail.com (J.T. Roehrig).
[1] Current address: University of Liverpool, Delby Street, Liverpool L69 3 GA, UK.

0042-6822/$ - see front matter Published by Elsevier Inc.
http://dx.doi.org/10.1016/j.virol.2013.03.011

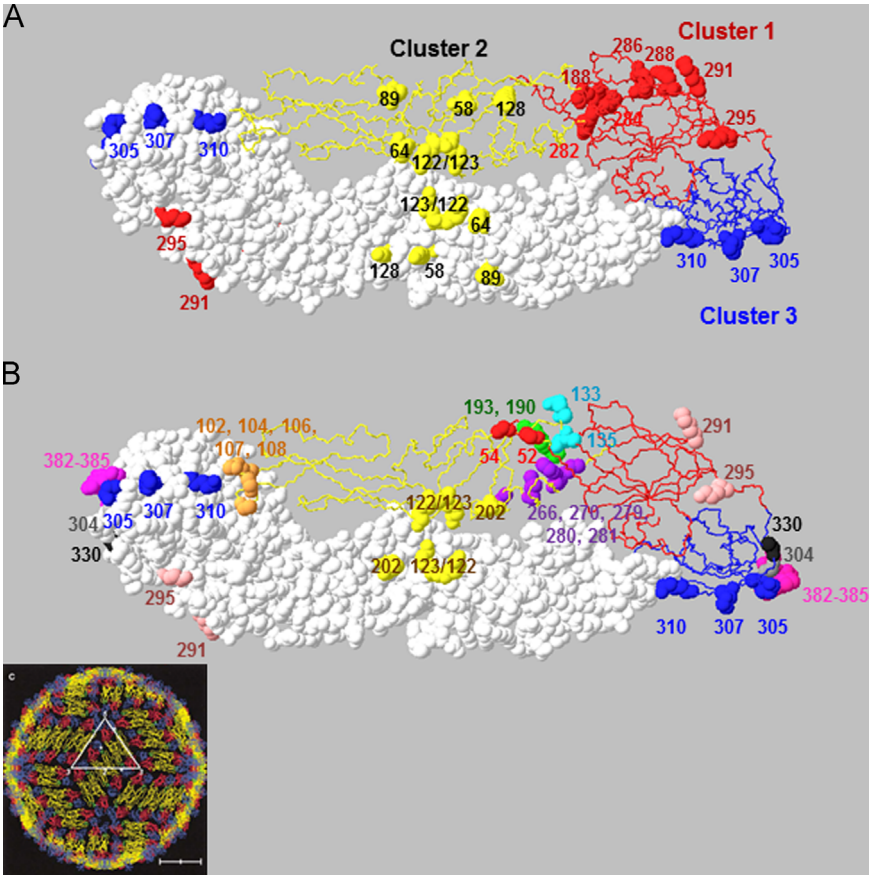

Fig. 1. Locations of HS-binding amino acid residues and mutations introduced in DENV2 E protein homodimers. Panel A: Location of possible HS-binding residues in the three potential binding clusters (Modis et al., 2003). Colors indicate locations in DI (red), DII (yellow) or DIII (blue). Panel B: backbone depiction of one monomer identifies locations of all mutations discussed. The DIII-FG (VEPG) loop mutants (dark pink), fusion peptide mutants (orange), and hinge region mutants (red, green, purple, and cyan) and have been previously described (Huang et al., 2010). Heparan sulfate-binding and DIII mutants (yellow, light pink, gray, and blue) and the G304K compensatory mutation G330D (black) described in this paper are also depicted. The second glycoprotein monomer is shown in a space-filling model to illustrate residue surface accessibility. The inset shows the configuration of homodimers in the surface of the virion (Kuhn et al., 2002). (For interpretation of the references to color in this figure legend, the reader is referred to the web version of this article.)

it exists – cannot be explained by interactions with only these AAs. Cell-specific interactions that result in differential DENV tissue-tropisms in vivo probably involve other plasma membrane receptors and potentially other E protein AAs. Several candidate cell membrane proteins have been shown to bind DENV in vitro but all are still poorly characterized (Martinez-Barragan and del Angel, 2001; Ramos-Castaneda et al., 1997). For example, it has been suggested that different cell surface proteins might be responsible for DENV binding to cultured monkey kidney cells (Vero) versus human hepatoma cells (HepG2) (Marianneau et al., 1996). Several size classes of mosquito cell (C6/36) membrane proteins appear to bind DENV, but these proteins also remain uncharacterized (Munoz et al., 1998; Salas-Benito and del Angel, 1997).

One surface protein, dendritic cell-specific intercellular adhesion molecule-3-grabbing non-integrin (DC-SIGN), has been well-studied as a flavivirus attachment protein (Boonnak et al., 2008; Davis et al., 2006a, 2006b). DC-SIGN binds to virion proteins containing mannose glycans, and appears to be involved in DENV infection of primary DCs or DC-SIGN-expressing transformed cell lines—primarily through the carbohydrate moiety at the N67 glycosylation motif of the E protein (Pokidysheva et al., 2006). Since oligosaccharides on mosquito cell-derived DENVs also contain high mannose glycans, attachment to DCs via DC-SIGN may be an important first step following mosquito-bite transmission of virus to humans (Hacker et al., 2009; Hsieh and Robbins, 1984).

The region of the E protein that might bind to cell-specific receptors remains controversial, partly because the virion surface glycoprotein contains no well-defined spike structures common to other enveloped viruses (Kuhn et al., 2002; Mukhopadhyay et al., 2003, 2006; Pletnev et al., 2001; Zhang et al., 2002). DIII was first hypothesized to contain the primary receptor-binding motif because DIII-reactive neutralizing monoclonal antibodies (MAbs), and to a lesser extent DI-reactive MAbs were most effective in blocking DENV attachment to and infection of Vero cells (Crill and Roehrig, 2001). MAbs against DII epitopes had measurable, but lower, blocking activity. Several other reports also suggest that DIII binds cellular receptors (Gromowski and Barrett, 2007; Modis et al., 2003, 2005; Roehrig et al., 1998; Sukupolvi-Petty et al., 2007; Thullier et al., 2001; Volk et al., 2007). Several AA changes in DIII result in phenotypic changes usually associated with viral attachment, e.g., host range, tissue tropism, or virulence, and DIII also contains the most effective virus neutralization sites (Jennings et al., 1994; Modis et al., 2005; Rey et al., 1995; Roehrig, 2003; Roehrig et al., 1998). For WNV, DII also elicits effective neutralizing antibodies in humans (Vogt et al., 2009).

Hung et al., demonstrated that soluble heparin blocked binding of recombinant DIII (EIII) of DENV2 E-protein to BHK-21 cells, but not to C6/36 cells(Hung et al., 2004). They also demonstrated that a peptide representing AAs 380–389 of DIII (containing the DIII-FG loop) inhibited binding of EIII to C6/36 but not BHK21 cells. These results suggested that DENV binding to mammalian and mosquito cells might be through different receptors. However, we have previously determined that a mutant DENV2 with a deletion of the DIII-FG loop (382VEPG385) was capable of infecting C6/36 cells,

Table 1
Amino acid variability in flavivirus E proein HS-binding motifs.

Virus[a]	HS-binding motif cluster 1[b]							HS-binding motif cluster 2[b,c]							HS-binding motif cluster 3[b,c]				
	1	2	2	2	2	2	2				1	1	1	2	3	3	3	3	3
	8	8	8	8	8	9	9	5	6	8	2	2	2	0	0	0	0	0	1
	8	2	4	6	8	1	5	8	4	9	2	3	8	2	3	4	5	7	0
DENV2 16681	R	H	K	R	R	K	K	K	K	R	K	K	K	E	T	G	K	K	K
DENV1 16007	R	H	K	R	K	K	K	K	K	N	V	T	K	K	T	G	S	K	K
DENV3 16562	R	H	K	R	K	K	K	K	K	N	L	E	K	K	L	S	S	V	K
DENV4 1036	R	H	K	K	R	K	K	T	S	Q	S	G	N	K	S	G	K	S	K
JEV																			
JaOArS982	R	H	K	R	K	K	K	S	S	S	T	S	R	G	T	E	K	S	K
WNV NY99	R	H	K	R	K	K	K	S	S	A	T	T	W	G	S	K	A	K	R
MVEV	R	H	K	R	K	K	K	N	T	N	S	N	R	G	T	E	K	T	K
SLEV MSI7	R	H	K	R	K	K	K	E	T	T	K	N	K	K	D	S	A	T	K
YFV Asibi	Q	H	K	R	K	A	K	K	V	D	A	K	F	E	T	D	K	S	K
TBEV																			
Neudoerfl	A	H	T	E	G	K	K	E	K	G	K	K	H	D	D	KT	K	T	R
LGTV TP21	A	H	T	E	G	K	K	E	K	G	K	K	H	D	D	KT	K	T	R
POWV LB	A	H	T	D	G	K	K	E	K	N	A	K	H	D	D	KT	K	K	R

[a] Accession numbers: U87411 (DENV2), AF180818 (DENV1), M18370 (JEV: Japanese encephalitis virus), AF196835 (WNV: West Nile virus), X03467 (MVEV: Murray Valley encephalitis virus), AY289618 (SLEV: St. Louis encephalitis virus), AY640589 (YFV: yellow fever virus), U27495 (TBEV: tick-borne encephalitis virus), AF253419 (LGTV: Langat virus), L06436 (POWV: Powassan virus).
[b] Amino acid positions of DENV2 E protein.
[c] Residues 202 and 303 are not basic residues in the HB-binding motif, but were targeted in this study to increase basic residues near the HB-binding cluster.

suggesting the DIII-FG loop is not the only or major receptor-binding site for C6/36 cells (Erb et al., 2010). Three basic residues, K305, K307, and K310, at a lateral ridge of DIII (DIII-A sheet in the E-dimer structure) were also speculated to form a potential HS-binding motif for DENV2 (Chen et al., 1997). A neutralizing epitope has also been mapped to K307 (Lin et al., 1994), suggesting these residues might be involved in viral attachment.

In an effort to gain a better understanding of mammalian cell attachment and entry, we report here the use of site-directed mutagenesis of a DENV2 infectious cDNA clone to introduce mutations in the HS-binding clusters and the DIII lateral ridge of the E protein. We evaluated the effects of these mutations on growth in mosquito and mammalian cells, membrane fusion in mosquito cells, attachment to Vero cells and DC-SIGN-expressing Raji cells, and expression of MAb-defined epitopes. Two Vero cell lethal mutants, KK291/295EV and KKK307/307/310EEE, were unable to initiate negative (−) sense viral (v)RNA synthesis in Vero cells by 72 h post-infection (p.i.), or replicate in DC-SIGN Raji cells, even though they were C6/36 cell-fusion competent, suggesting that these mutations abrogate an early step in viral replication, prior to virus-mediated endosomal membrane fusion. Additionally, both of these mutant viruses failed to react with MAbs shown previously to block DENV attachment to Vero cells.

Table 2
Growth of DENV2-16681 E-protein mutant viruses in C636 and Vero cells and resultant E-gene sequence of progeny virus.

Mutant viruses[a]	Virus titer ($TCID_{50}$/ml)[b]		% Fusion[d]
	C6/36	Vero	
KK122/123EE	8.63 ± 0.2	Lethal (TS)[c]	
└> **K122E** (*V1*)	9.13 ± 0.5	6.75 ± 0	85 ± 16
KKK122/123/128EEE	Lethal	Lethal	N.d.
KRR284/286/288EEE	Lethal	Lethal	N.d.
KK291/295EE	Lethal	Lethal	
└> **KK291/295EV** (*C0*)	7.25 ± 0	Lethal (TS)	84 ± 10
KKK305/307/310EEE	7.25 ± 0	Lethal	90 ± 5
E202K	7.63 ± 0.2	Lethal	
└> **E202K**+**K122E** (*V1*)	n.d.	6.5 ± 0	54 ± 5
G304K	9.38 ± 0.2	Lethal	
└> **G304K**+**G330D** (*V1*)	n.d.	6.25 ± 0	84 ± 14
30P-NBX (DENV2 16681)	9.63 ± 0	7.38 ± 0.2	100

[a] Bold-letters and arrows indicate amino acid changes associated with transfection (0) or one passage (1) in Vero (*V*) or C6/36 (*C*) cells. Mutations were identified by sequencing viral RNA from Vero cells at 12 days p.i.
[b] Peak infectious viral titer in growth curve ($n=2$); n.d.=not done.
[c] TS=temperature sensitive: mutant virus was able to grow to similar titer as the 30P-NBX in Vero cells at 28C without acquiring any compensatory mutation.
[d] Average percent fusion (±s,d,) of C6/36 cells fused with 30P-NBX positive control ($n=2$–5).

Results

Mutant virus growth in different cell types

Location of the E protein HS-binding clusters is shown in Fig. 1A. The flavivirus AA variability of all clusters is shown in Table 1. Based on these data, seven new DENV2 mutants targeting the putative HS-binding motifs or DIII-A receptor binding motifs in the viral E protein were prepared (Tables 1 and 2). Five mutations were at basic AA residues, which were converted to acidic residues, e.g., K/R→E. Residue 202, located in HS-binding cluster 2, is a basic K in DENV serotypes 1, 3, and 4, but it is acidic E for DENV2 (Table 1). Therefore, an E202K mutation was made to determine whether the additional basic residue for DENV2 in this cluster is advantageous. Finally, a G304K mutation was made at the DIII lateral ridge to increase the overall basic characteristics of the DIII-A sheet.

From these 7 mutations, we recovered 5 viable mutant viruses following transfection of C6/36 cells. Four mutants were as designed: KK122/123EE, KKK305/307/310EEE, E202K, and G304K (Table 2). Transfection of C6/36 cells with KK291/295EE-encoding RNA resulted in isolation of a virus with KK291/295EV mutations. The full-length viral genome sequence of each C6/36 working seed virus was completed and with the exception of KK291/295EE→KK291/295EV, only the introduced mutations were found.

Three of the mutant viruses were unable to grow in Vero cells without subsequent modification. Transfection of or a single passage in Vero cells of the KK122/123EE mutant resulted in the isolation of a K122E virus, where the engineered E123 mutation reverted to K123. A single passage of the E202K mutant in Vero

cells resulted in isolation of viruses with either a reversion to E202, or acquisition of a second compensating mutation, K122E, in virus where the E202K mutation was conserved. A single passage of G304K in Vero cells resulted in isolation of a mutant virus containing an additional compensatory mutation, G330D. Most of the reversions and/or compensatory substitutions were reproducible in 2–3 independent experiments to derive/amplify the mutant viruses from Vero cells. The triple mutant, KKK305/307/310EEE, and double mutant, KK291/295EV, were lethal for growth in Vero cells. The KK291/295EV mutant was, however, able to grow to very low titers in HepG2 ($2.3\log_{10}$ $TCID_{50}$/ml) and K562 ($2.4\log_{10}$ $TCID_{50}$/ml) cells. The KKK122/123/128EEE, KRR284/286/288EEE, and KK291/295EE mutations were lethal in all cell types. The locations of the HS binding and DIII mutations from which live virus were rescued are depicted in the E protein backbone diagram in Fig. 1B. Since attachment of our previously published mutant viruses is evaluated here, we have included the fusion peptide, hinge region, and DIII-FG loop mutants in Fig. 1B (Butrapet et al., 2011; Huang et al., 2010). Locations of all mutations are also depicted on a space-filling monomer to show their surface accessibility.

To characterize the phenotypes of these mutants, we prepared growth curves in Vero and C6/36 cells based on genomic equivalent titers by qRT-PCR (data not shown), and determined the peak infectious virus titers between day 8 and 14 pi based on the $TCID_{50}$ titers (Table 2). The clone-derived 30P-NBX virus was used as a parental DENV2 16881 control throughout the experiments. We used qRT-PCR to quantify the vRNA in culture medium (data not shown) along with the $TCID_{50}$ titer to monitor the infectivity of mutant viruses. In C6/36 cells the KK291/295EV, KKK305/307/310EEE, and E202K mutant titers were about 100-fold lower than the 30P-NBX parental virus. The K122E and G304K mutant viruses grew to similar levels as 30P-NBX. All viruses reached highest GE titers by day 8 p.i. in C6/356 cells. Peak infectious titers ($TCID_{50}$/ml) were on day 12 pi (Table 2). Mutant viruses that contained compensatory mutations permitting replication in Vero cells, K122E, E202K/K122E, and G304K/G330D, had ~4- to10-fold reductions in titers as compared to 30P-NBX in Vero cells. The K122E mutant had similar growth kinetics (maximum GE titers between day 8 and 12 p.i.) to wt virus and peak infectious titers on day 8 pi. The peak infectious titers of K202K/L122E and G304K/G330D were on day 12 pi (Table 2).

We also investigated the effect of temperature on growth of the 5 mutant viruses by comparing the growth in Vero cells at 37C and 28C at 4 days p.i. (data not shown). While all mutants grew to some extent in Vero cells at 28C, only the KK122/123EE and KK291/295EV mutants grew to the same level as 30P-NBX at 28C while retaining the correct mutations in their progeny virus, thus qualifying them as temperature sensitive (TS) in Vero cells (Table 2).

Virus-mediated fusion of C6/36 cells

We have shown previously that mutation of the E protein fusion peptide and hinge region results in viruses unable to grow in Vero cells. This loss of growth in mammalian cells was correlated with a defective virus-mediated fusion process in C6/36 cells (Butrapet et al., 2011; Huang et al., 2010). Mutation of the DIII-FG loop (VEPG382) did not result in a loss of fusion activity (Erb et al., 2010). Fig. 2 compares all mutant viruses tested to date for their growth in Vero and C6/36 cells, and their ability to mediate membrane fusion in C6/36 cells. Table 2 gives specific average values and standard deviations for only the new HS mutants. For the new mutations reported in this study, the only stable mutants, KK291/295EV and KKK305/307/310EEE, failed to grow in Vero cells while maintaining fusion activity in C6/36 cells (Fig. 2, arrows).

Epitope-binding analyses of mutant viruses

MAb-reacting epitopes of mutant E proteins were mapped by IFA using acetone-fixed, virus-infected C6/36 cells and a subset of MAbs known to react with each domain of the E protein (Table 3). Four-fold or greater differences in reactivity compared to 30P-NBX virus were considered significant changes in reactivity. No mutations

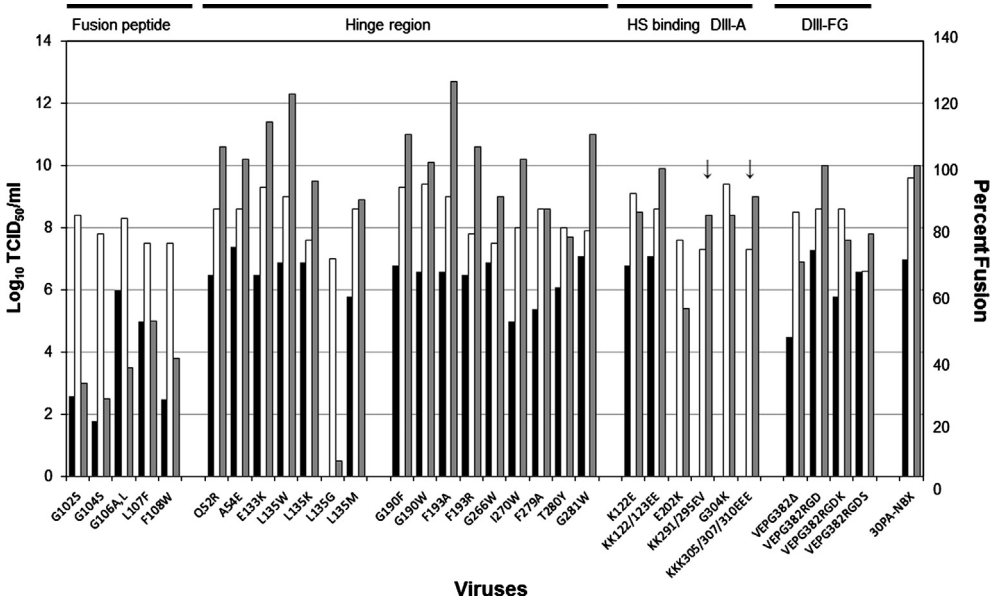

Fig. 2. Functional arrangement of E protein mutations yielding viable virus. The relative growth of viruses (log $TCID_{50}$/ml) measured at peak titer (12–14 days p.i.) is shown for virus-infected Vero (black bars) and C6/36 (white bars) cells (left *y*-axis). Also shown is percent fusion of each mutant virus as compared to the 30P-NBX wild-type virus (100%) (gray bars) (right *y*-axis). Arrows identify mutants that do not grow in Vero cells but are fusion competent in C6/36 cells. Bars represent mean values ($n=3$). Growth and fusion data from the fusion loop, hinge region, and VEPG (DIII-FG) mutants have been published previously (Butrapet et al., 2011; Erb et al., 2010; Huang et al., 2010). Specific averages and standard deviation for the new HS mutants are given in Table 2.

Table 3
MAb epitope mapping of viruses containing mutant E-proteins determined by IFA end-point titration on virus-infected C6/36 cells.

Virus	E protein						prM protein
	Domain I	Domain II		Domain III			
	C1[a]	A1	A4	B1	B2	B	
	1B4C-2[b]	6B6C-1	2H3	3H5	9A3D-8	1A1D-2	2H2
30PA-NBX	0.12[c]	0.12	0.63	0.31	1.88	0.24	0.12
K122/123E	0.12	0.12	0.63	0.63	1.88	0.24	0.12
K122E	0.12	0.12	0.63	0.63	1.88	0.24	0.12
KK291/295EV	**0.47**[d]	0.12	1.88	0.47	1.88	0.26	0.12
K305/307/310E	0.12	0.12	0.94	**>10**	**>10**	**7.5**	0.12
E202K	0.12	0.12	1.25	0.47	1.88	0.24	0.12
G304K	0.24	0.12	0.47	0.63	1.88	0.12	0.12

[a] Epitope (Roehrig et al., 1998).
[b] MAb (Roehrig et al., 1998).
[c] End-point MAb titer expressed in μg/ml, result is average from 3 to 4 experiments.
[d] Bold/underlined values indicate 4-fold or greater differences in end-point titers compared to wild-type virus, 30P-NBX.

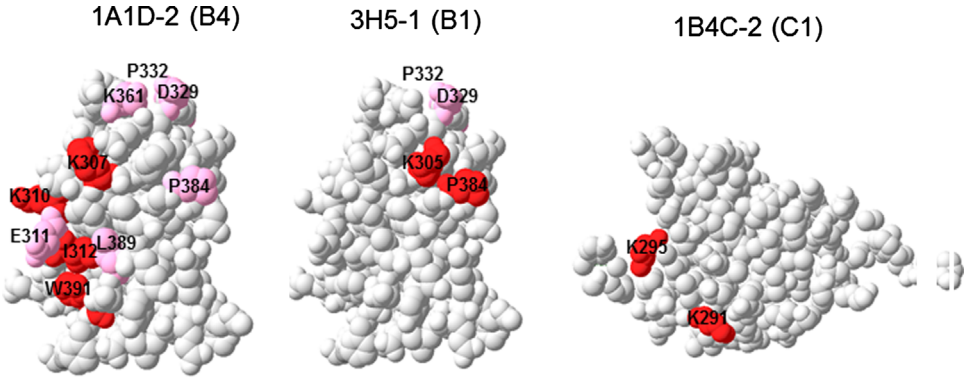

DIII Mutant	RxN
G304K	+
K305/307/310	-
VEPG382Δ	+
VEPG382RGD	+
VEPG382RGK	+
VEPG382RGDS	+

DIII Mutant	RxN
G304K	+
K305/307/310	-
VEPG382Δ	-
VEPG382RGD	-
VEPG382RGK	-
VEPG382RGDS	-

DI Mutant	RxN
L133K	+
L135G	-
L135W	+
L135M	+
L135K	-
KK291/295EV	-

Fig. 3. Epitope mapping of DENV2 E protein mutants using three anti-DENV mouse MAbs. Space-filling models of portions of DIII (left and center) and DI (right) of the DENV E protein are shown with the MAb that binds to that epitope indicated above. The AAs known to be highly critical for MAb binding (red), and accessory binding AAs (pink) in each epitope are indicated. The DENV epitope identified by each MAb is shown in parentheses (Roehrig et al., 1998). Reactivity with MAb of relevant mutant viruses is shown in the lower tables. (For interpretation of the references to color in this figure legend, the reader is referred to the web version of this article.)

altered the binding of DII-reactive MAbs. The mutant KK291/295EV in DI lost reactivity with MAb 1B4C-2 (epitope C1). We showed previously that the C1 epitope was also lost following a L135G mutation (Butrapet et al., 2011). The DIII mutant KKK305/307/310EEE lost reactivity with MAbs 3H5, 9A3D-8, and 1A1D-2. These MAbs define DIII epitopes B1, B2, and B4, respectively. We showed previously that all four VEPG mutants also lost reactivity with 3H5 (*B1*) (Erb et al., 2010). A summary of the MAb/mutant reactivity is shown in Fig. 3, including locations of other AAs previously shown to be involved in the binding of 1A1D-2 and 3H5 (Lok et al., 2008; Sukupolvi-Petty et al., 2007). The last panel shows the locations of K291 and K295 in DI, which are involved in the binding of 1B4C-2. The location of L135 is not shown in the 1B4C-2 (C1) panel, although the L135G mutation was previously shown to disrupt binding, since it is located in the E protein hinge region and is not surface accessible.

Virus attachment to Vero cells using detection of vRNA by qRT-PCR as a virion surrogate

It has been reported previously that DENV2 attachment to cell receptors is non-saturable. These previous studies used radioactively-labeled virus and LLC-MK_2, Vero, C6/36, AP61, and Huh-7 target cells (Hilgard and Stockert, 2000; Thaisomboonsuk et al., 2005). Non-saturable binding kinetics may indicate non-specific binding. We repeated the Vero cell attachment assay using 30P-NBX parental virus and qRT-PCR to detect bound/free vRNA. Using this technique, we confirmed the non-saturable kinetics of DENV2 attachment to Vero cells using MOIs of 1, 10, or 100. In each case, approximately 10% of input virus bound to cells regardless of MOI (data not shown). Similarly, when the time course of attachment was measured, the overall rate of attachment was similar regardless of viral input (Fig. 4), further suggesting non-saturable

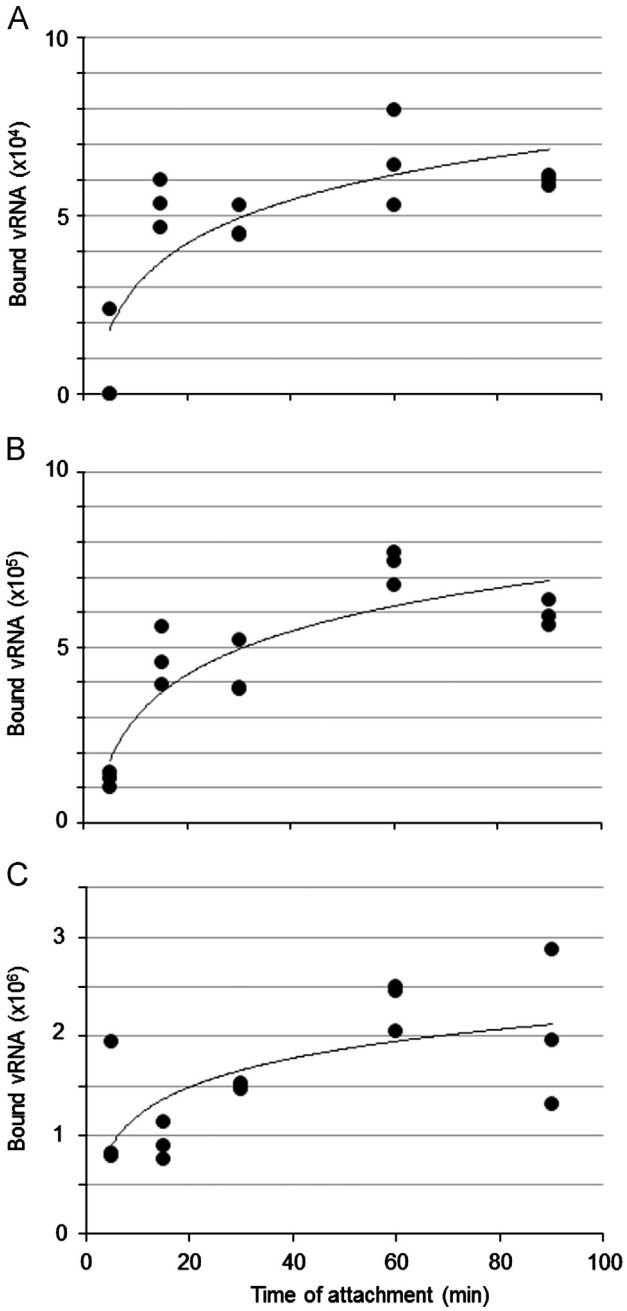

Fig. 4. Attachment curves of DENV2 30P-NBX to Vero cells at varying MOI. Parental/wild type virus, 30P-NBX at indicated MOI was allowed to attach to Vero cell monolayers at 4C and at indicated times cells were rinsed, harvested, and attached DENV vRNA was measured by qRT-PCR. Panel A, MOI=1; panel B, MOI=10; and panel C, MOI=100.

kinetics. In an attempt to improve the specificity of viral attachment to cells we used a variety of techniques, e.g., treating cells with trypsin or trypsin/RNase or trypsin/RNase/proteinase K post-attachment to remove non-specifically bound virus and vRNA. None of these techniques improved attachment specificity even if protease treatment occurred after allowing time for internalization (2 h incubation at 37C post-attachment, data not shown). Because of these results, we did not to use attachment/qRT-PCR assay to measure viral attachment.

Blocking viral attachment with heparin

Virus attachment to cells was further investigated in a heparin inhibition experiment. As shown in Fig. 5, binding of w.t. 30P-NBX

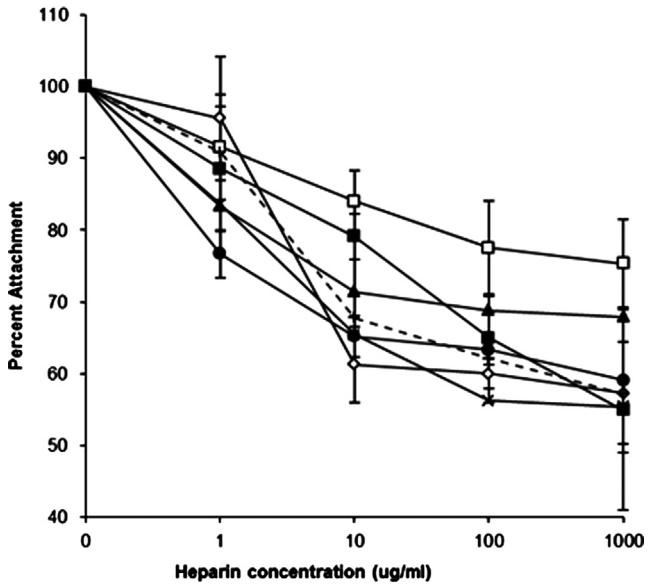

Fig. 5. Competition for viral attachment to HepG2 cells with increasing concentrations of heparin. Average percent reduction in viral attachment to HepG2 cells measured by cell-associated vRNA ($n=3$). Viruses: 30P-NBX (◇), KK122/123EE (□), K122E (▲), KK291/295EV (X), KKK305/307/310EEE (■), E202K (●), and G304K (+, dotted line). Standard error bars are shown.

and mutant viruses to Hep-G2 cells could be inhibited up to 40% in a dose-dependent manner by incubating with heparin. Only KK122/123EE and K122E mutants were significantly less susceptible ($p < 0.05$, unpaired t-test) to heparin inhibition relative to wt 30 P-NBX virus at dose of 100 ug/ml (both mutants) or 1000 ug/ml (onlyKK122/123EE).

Measuring negative (−) vRNA synthesis in virus-infected Vero cells as an indication of virus replication in Vero cells

We previously measured virus attachment to Vero cells using plaque assay (Crill and Roehrig, 2001). In that study, we used 100 plaque forming units (PFUs) in the attachment assay and by counting plaques at 5 days p.i., we could calculate the percent viral attachment that resulted in a viable infection, i.e., plaque formation. We believe that this is the best system for performing attachment assays; however, because many of our mutant viruses were not able to grow in Vero cells, an assay that relied on viral PFUs was not feasible.

Another method to determine the point at which entry-lethal mutations block replication is to quantify production of (−) strand vRNA post-attachment. The reasoning is that for (+) vRNA viruses, if a virus genome contains a lethal mutation that blocks initiation of (−) vRNA synthesis, yet is fusion competent, the replication block must occur prior to virion endocytosis, thus implying an early block in viral entry, at least prior to fusion with endosomal membranes.

We performed these (−) vRNA synthesis studies by adsorbing 1×10^4 $TCID_{50}$ of DENV2 to Vero cells at 4C for 1 h, washing off non-attached virus, and detecting initiation of replication by measuring intracellular levels of (−) vRNA at 72 h post-attachment (Fig. 6A). We compared levels of intracellular (−) vRNA to viral growth by measuring extracellular (+) vRNA at 4 and 72 h post-attachment (Fig. 5B). Not surprisingly, Vero cells infected with mutant viruses shown previously to be defective in membrane fusion activity (Fig. 5A, mutants G104S, F108W, E133K, and L135G) had no measurable intracellular (−) vRNA or viral growth. The mutants that were fusion competent but failed to initiate (−) vRNA synthesis in Vero cells were E202K, KK291/295EV, KKK305/307/310EEE, VEPG382Δ, and VEPG382RGDK (Fig. 6A). Viral

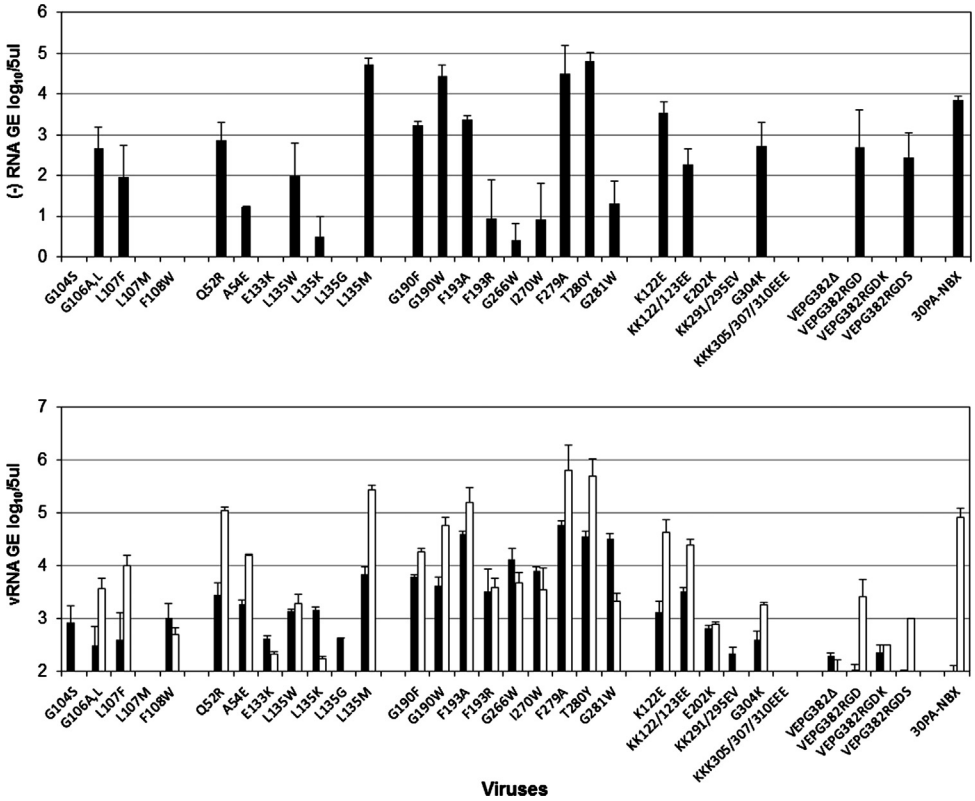

Fig. 6. RT-qPCR quantitation of viral genomic equivalents for mutant DENV following a 1 h attachment to Vero cells at 4 °C. 1×10^4 $TCID_{50}$ mutant DENV2 was adsorbed to Vero cells at 4C for 1 h, unattached virus was removed by washing. Five μl of extracted intracellular (−) vRNA) or extracellular (+) vRNA) was quantitated using qRT-PCR. Panel A: intracellular (−) vRNA measured at 72 h p.i. Panel B: extracellular (+) vRNA measured at 4 h (black bars) and 72 h (white bars) p.i. Data are reported as mean and standard error of the mean ($n=3$).

mutants that had previously been found unable to grow in Vero cells also showed little or no growth in these experiments as determined by measuring extracellular levels of vRNA at 4 h and 72 h p.i. (Fig. 6B). As an additional control to this approach, we measured levels of (−) vRNA in C6/36 cells infected with 30P-NBX and the HS-binding/DIII mutants. All that were able to grow in C6/36 cells expressed (−) vRNA at levels comparable to 30P-NBX except for the triple mutant virus KKK305/307/310EEE. The level of (−) vRNA in the triple mutant-infected C6/36 cells was about 10-fold less (1×10^5 vs. 1×10^6 genomic copies) than the other viruses, consistent with its reduced replication in C6/36 cells (data not shown).

Infection of DC-SIGN transformed Raji cells

To analyze if the KKK305/307/310EEE or KK291/295EV viruses could infect a mammalian cell line with a known alternative attachment protein that did not rely on a heparan sulfate interaction, we compared the ability of mutant viruses and wild-type 30P-NBX virus to infect Raji cells with and without DC-SIGN on the surface. The Raji/0 cells are refractory to DENV, however Raji-DC-SIGN cells can be infected. The interaction of DENV and DC-SIGN has been shown previously to be mediated by the carbohydrate at the N67 glycosylation site of the E-protein (Pokidysheva et al., 2006). For these experiments we also included the fusion peptide mutant G104S, shown previously to be defective in membrane fusion, as a negative control virus. After a 1 h attachment at 4C, we monitored viral growth by immunofluorescence of infected cells and qRT-PCR of progeny virus vRNA at 72 h p.i. By both methods the 30P-NBX replicated only in Raji-DC-SIGN cells in a dose-dependent manner (Fig. 7). None of the mutants infected either Raji/0 or Raji-DC-SIGN cells.

To determine if the introduced mutations had an effect on E protein glycosylation, wild-type 30P-NBX, the two DIII mutants, KKK305/307/310EEE and KK291/295EV, and the DII mutant, G104S, mutants were concentrated from virus-infected cell culture medium by anti-E protein affinity chromatography with MAb 4G2, prior to treating with either endoH or PNGase F Not surprisingly, the resulting glycosidase treated virus E protein electrophoretic gel profiles were identical for all four viruses, indicating two oligosaccharide structures on the E-protein - one being an endoH susceptible mannose glycan (presumably N67) and one site being an endoH resistant complex glycan (N153) (data not shown). These results are similar to results from other studies (Hacker et al., 2009)

Discussion

The flaviviral E protein mediates at least two crucial aspects of infection—attachment and cell membrane fusion. We have identified E protein AA sequence elements required for these critical functions using mutant viruses obtained by transfection of C6/36 cells with DENV2 genome RNA transcribed from infectious cDNA clones. Our previous studies identified the fusion peptide region and the hinge region of the E protein as being critical for virus-mediated membrane fusion in C6/36 cells and growth in Vero cells (Butrapet et al., 2011; Huang et al., 2010). In this study we mutated proposed surface accessible HS-binding motifs in DENV2 E protein DI, II and III, including AAs in the lateral ridge of DIII-A strand, and assessed the effects of these mutations on viral phenotype.

Two triple mutations, KKK122/123/128EEE and KRR284/286/288EEE, were lethal in both C6/36 and Vero cells, so no progeny viruses were obtained post-transfection, and these mutants were not further studied. The KK291/295EE mutant was also unable to

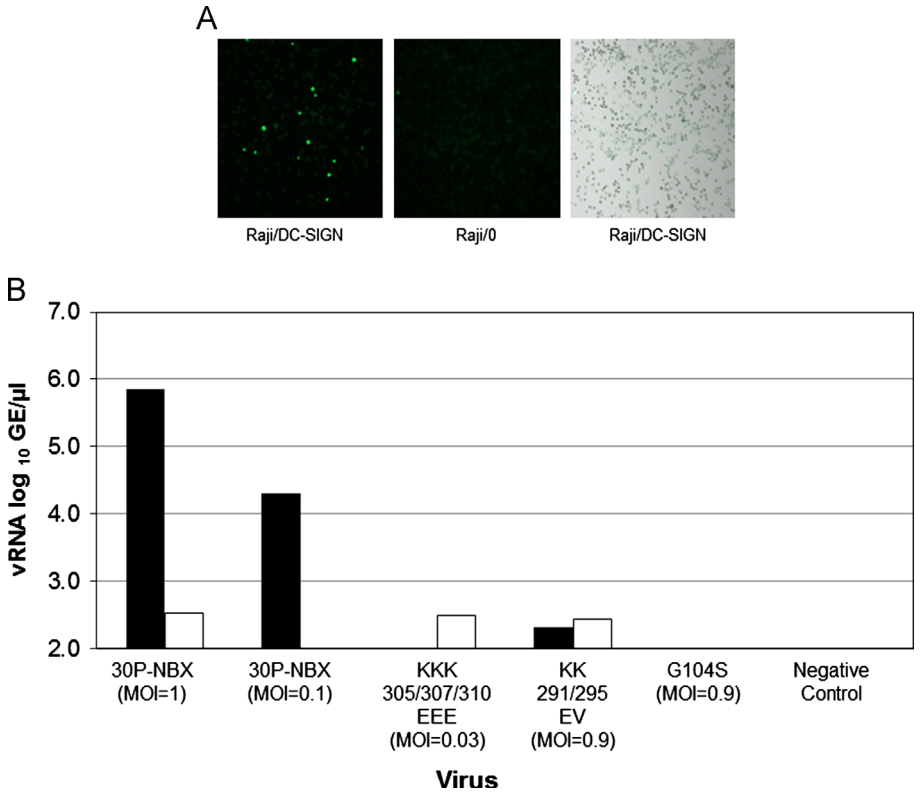

Fig. 7. Growth of 30P-NBX and mutant viruses in Raji cells and DC-SIGN-transformed Raji cells. Viruses were attached to cells for 1 h at 4C, and unattached virus was removed by rinsing in PBS. Four days p.i., cells were stained for expression of DENV2 antigens, and progeny virus genomes were quantitated by qRT-PCR. Panel A, IFA staining of cells with DENV-2 polyclonal antibody; in order left to right: Raji-DC-SIGN cells infected with 30P-NBX (positive), Raji cells infected with 30P-NBX (negative), and light microscopy of Raji/DC-SIGN cells to show cell density on slide. Change in genomic equivalents of 30P-NBX and mutant viruses from $T=0$ to $T=72$ h p.i. Raji/DC-SIGN cells (■) and Raji/0 cells (□). A representative result is shown ($n=3$).

grow in C6/36 cells unless a compensatory E295V mutation was acquired (Table 2). While all other mutants, KK122/123EE, KK291/295EV, KKK305/307/310EEE, E202K, and G304K, grew in C6/36 cells, their biology changed dramatically when grown in mammalian Vero cells, where most mutations were lethal. Mutants K122/123E, E202K, and G304K required compensatory modifications for growth in Vero cells. All three of these modified viruses were fusion competent in C6/36 cells in addition to growing in Vero cells (Fig. 2).

The list of mutant viruses that retained viability suggested that the highly DENV- and JEV-serogroup conserved K or R basic residues at positions 282, 284, and/or 288 in the DI-HS-binding cluster are essential for virus function in both C6/36 and Vero cells. It should be noted that for HS cluster 1, structural analyses of the E homodimer suggest that residues R188, H282, K284, R286, and H288 are not readily accessible on the surface of the virion. The buried location of most of these AAs might explain the overall AA conservation of cluster 1 among flaviviruses. The other highly conserved residue in the DI-HS-binding cluster, K295, is also critical and changing it to E295 resulted in lethality or instability in both cell types. Both K291 and K295 are accessible on the virion surface (Fig. 1). Substitution of the basic K295 to neutral V295 was tolerated by C6/36 cells, but not by Vero cells. When comparing the viability of viruses with the single, double and triple mutations of K→E at the 122/123/128 residues in the DII-HS-binding cluster (Table 2), it appears that the K128 (Table 1) is the most critical determinant for viability in both cell types. On the other hand, the K123E mutation mainly affected temperature sensitivity of the virus at 37C (KK122/123EE was able to replicate in both C6/36 and Vero cells at 28C). Another mutant, KK291/295EV, exhibited the temperature sensitive phenotype at 37C in Vero cells, implying that a charge change at positions 123, 291, and/or 295 may cause a structural instability of the E protein at 37C that might affect either E protein intracellular processing or viral attachment.

Interestingly, the E202K and G304K mutations are not stable in Vero cells, and compensatory mutations K122E and G330D, respectively, evolved during virus replication. Both the E202 and K122, and the G304 and G330 residue pairs are spatially close in the E protein (Fig. 1), and the compensatory mutations would have reduced the overall positive charges in the DII-HS-binding cluster or DIII A strand to the same levels as the parental 30P-NBX virus. These results suggest that the overall positive charges of these two clusters might be critical for proper DENV2 infection in mammalian cells.

The K122E compensatory mutation that occurred during replication of E202K mutant in Vero cells has previously been observed to evolve (K→E or I substitution) with other DENV2 E mutants when grown in Vero cells (e.g., E133K, G266W, I270W, VEPGΔ, and VEPG382RDGK) (Butrapet et al., 2011; Erb et al., 2010). Additionally, the 16681 parental virus spontaneously accrued the K122E mutation after multiple Vero cell passages (data not shown). These observations suggest that change of the K122 in DENV2 to a non-basic AA might represent a Vero cell-adaptation. We have also found that the K122E adaptation greatly enhances the ability of 30P-NBX to infect *Aedes aegypti* mosquito midguts (Erb et al., in preparation).

Two mutant viruses – KK291/295EV and KKK305/307/310EEE – were lethal in Vero cells, but fusion competent in C6/36 cells (Fig. 2). Because of this, we turned our attention to ascertaining the replication block for these two viruses in Vero cells. Previous attachment studies using radioactively-labeled virus demonstrated that DENV attachment to a variety of cell types is non-saturable (Hilgard and Stockert, 2000; Thaisomboonsuk et al., 2005). We confirmed those observations using qRT-PCR to detect attached vRNA as a surrogate for virus. When virus attachment

time-course experiments at 4C were performed, reasonable curves were generated (Fig. 4); however, the attachment curve kinetics, and percent viral attachment (10%), did not change over a wide range of MOIs, further suggesting non-saturable binding kinetics. The inability to saturate viral binding sites on Vero cells is perplexing. One explanation could be that non-specific binding is high. Experiments designed to reduce non-specific binding failed to do so. Regardless of this fact, not unexpectedly, attachment of all viruses to mammalian cells could be reduced by previous incubation of virus with heparin (Fig. 5). This competition was seen in all viruses tested, likely because for each mutant, other HS-binding sites were still present on the glycoprotein. Only KK122/123EE and K122E became less susceptible to high dose of heparin inhibition than the 30P-NBX virus, suggesting the basic residues at 122 and 123 might be a dominant cluster for HS binding.

Another perplexing observation is that it has been suggested that DENV attachment is most efficient at pH values below the threshold necessary to catalyze the oligomeric reorganization of the E homodimer to a fusion-competent E homotrimer (pH 5.5–6.0) (Hilgard and Stockert, 2000; Thaisomboonsuk et al., 2005). It is unclear how a virion with E proteins in a fusion-ready homotrimer would interact with the cell surface. Additionally, it has been shown previously that when a flavivirus is exposed to low pH, it is inactivated (Guirakhoo et al., 1993). Because of these observations, it is not clear what was being measured in low pH attachment assays. Because most of our mutations resulted in surface charge changes that could affect each mutant virus's binding in different ways, we elected to conduct our attachment assays at the physiological pH of 7.4.

Another factor that all previous binding studies have in common is the failure to assess directly the ratios of prM/M in virions. Virions with either uncleaved prM or with prM pre-peptide still associated might have an altered attachment phenotype. Because our viral seeds were produced in C6/36 cells we assume that all viruses have some prM on their surfaces, since it has been observed that flaviviruses produced from C6/36 cells contain high proportions of prM (Randolph et al., 1990; Zhang et al., 2003). Protein gel analysis of the KKK305/307/310 mutant virus confirmed the presence of prM in the virion (data not shown).

Because of these caveats and our inability to establish a reliable attachment assay, we used post-attachment synthesis of intracellular (−) vRNA as a surrogate for viral attachment that leads to infection. Mutant viruses that failed to produce (−) vRNA by 72 h p.i. were G104S, L107M, F108W, E133K, L135G, E202K, KK291/295EV, KKK305/307/310EEE, VEPG382Δ, and VEPG382RGDK (Fig. 6A). Not surprisingly, we also found that these mutants did not grow well in Vero cells at 72 h p.i. (Fig. 6B). Four of these mutants, G104S, L107M, F108W, and L135G, were shown previously to be fusion-negative so these mutations are lethal for Vero cells. Four other mutants, E133K, E202K, VEPG382Δ, and VEPG382RGDK, required reversion or compensatory mutations before they could grow in Vero cells. The growth of these four mutants was readily observed at 12 days p.i. (Table 2 and Fig. 2), so their failure to produce (−) vRNA by 72 h p.i. is probably associated with the longer time necessary to accrue and select for the rescuing mutations.

The KK291/295EV and KKK305/307/310EEE mutants were fusion competent in C6/36 cells, but neither production of (−) vRNA nor viral growth could be detected in Vero cells (Fig. 2A, and Fig. 6B). Because these two mutations also resulted in loss of reactivity with MAbs that have been shown to block attachment of virus to Vero cells, it is likely that these viruses are not able to attach to Vero cells (Crill and Roehrig, 2001). As discussed above, the KK291/295EV mutant is temperature sensitive. Since our viral attachment assays were performed at 4C, the inability of mutant KK291/295EV to attach to Vero cells is not related to E protein conformational changes that might occur at 37C. Besides the MAbs tested here, the epitope recognized by MAb 4E11, which strongly neutralizes all DENV, has also been mapped to this region, AAs 304–314 (Thullier et al., 2001). Our analysis does not differentiate loss of attachment caused by the loss of a HS-binding site from loss of binding to a virus-specific receptor in DIII. Either or both mechanisms could be in play here, because the conserved HS-binding residues K305, K307, and K310 are located in DIII.

To evaluate attachment in another way, we tried to grow the KK291/295EV and KKK305/307/310EEE viruses in Raji cells expressing DC-SIGN on their surface. Previous studies have identified the carbohydrate at the N67 of the E protein as the moiety involved in DC-SIGN-mediated attachment. DENV infection of DC-SIGN-bearing cells can be inhibited by chemicals that block acidification of endosomes (e.g., bafilomycin and chloroquine), suggesting that DENV entry into these cells requires membrane fusion (Navarro-Sanchez et al., 2003; Thullier et al., 2001). Because both the KK291/295EV and KKK305/307/310EEE mutants have normal fusion activity in C6/36 cells, we predicted that these mutants would infect DC-SIGN-bearing mammalian cells, however neither of these mutants nor an additional mutant, G104S (shown previously to be defective in cell membrane fusion) infected Raji-DC-SIGN cells, despite w.t. virus glycosylation patterns. Interestingly, the spread of DENV in infected Raji-DC-SIGN cells was less than that seen in DENV-infected Vero cells, confirming a previous study (Navarro-Sanchez et al., 2003). These results suggest that there is another, as yet undefined attenuating step in DENV infection of Raji-DC-SIGN cells.

Another alternative DENV entry mechanism is via Fc-receptors on the cell surface after the virus is complexed with non-neutralizing antibody. Additionally, it has recently been shown that DENV can be labeled directly with fluorescent dyes (Zhang et al., 2010). These tagged viruses can be used to evaluate viral attachment. We are currently using both approaches to expand our understanding of the early events in DENV2 replication.

Materials and methods

Site-directed mutagenesis, construction of infectious cDNA clones and production of mutant viruses

Mutant genomic cDNAs of DENV2 were constructed using the pD2/IC-30P-NBX plasmid (30P-NBX) containing full-length genomic cDNA of DENV2, strain 16681, as previously described (Butrapet et al., 2011; Erb et al., 2010; Huang et al., 2010). Mutant viral RNA (vRNA) was transcribed in vitro from linearized full-length cDNA, and the transcribed-RNA was transfected by electroporation of C6/36 or Vero cells. Working seed virus for each mutant was obtained by one passage of the mutant virus in either Vero or C6/36 cells. Full-length genome consensus sequencing of viral seeds was performed to confirm the final genome sequence of recovered mutants from each cell type.

Fifty percent tissue culture infectious dose ($TCID_{50}$) assay

Virus infectivity titer was measured by $TCID_{50}$ assay since some of these mutants were unable to grow in Vero cells (Bryant et al., 2007). Briefly, C6/36 cells in 96-well tissue culture plates were infected with serially diluted virus. Following incubation at 28C for 12 days, the plates were fixed with acetone, and viral antigens were detected by enzyme-linked immunosorbent assay (ELISA) using DENV2—mouse hyperimmune ascitic fluid (MHIAF). The $A_{405\ nm}$ was measured, and $TCID_{50}$ titers were calculated using the Reed–Muench method.

Growth studies of mutant viruses in cell culture

Vero, K562, HepG2, and C6/36 cells were cultured as previously described (Butrapet et al., 2011; Huang et al., 2010). Cell cultures in 75-cm^2 flasks were infected with mutant viruses in duplicate at a multiplicity of infection (MOI) of 0.001 $TCID_{50}$/cell. Vero cell cultures were also used to test temperature sensitivity of the mutants when replicated at 28C and 37C. Culture medium aliquots were removed from each flask every other day during 12 (for Vero) or 14 days (C6/36) of culture incubation. Viral particles in the medium were first quantitated by measuring the genomic equivalents (GE) of vRNA using one-step quantitative (*q*) RT-PCR. The vRNA was extracted with QIAamp Viral RNA kit (Qiagen), and qRT-PCR was conducted with iScrip one-step RT-PCR kit (BioRad) or Quantitect virus kit (Qiagen) in the iCycler iQ5 (BioRad) with the following protocol: 50C for 30 min and 95C for 15 min followed by 45 cycles of 95C for 15 s and 60C for 1 min. Primers/probe for the qRT-PCR were universal DENV-10578 (AAGGACTAGAGGTTAGAGGAGACCC), universal CDEN-10687 (GGCGTTCTGTGCCTGGAATGATG), and D24-10616 FAM probe (AACAGCATATTGACGCTGGGAAAGACC). DENV vRNA fragments were in vitro transcribed from a DENV2 cDNA subclone, quantitated by RiboGreen RNA quantification kit (Molecular Probe), and serially diluted to desired GE to generate the standard curve for each one-step qRT-PCR assay. Only results for assays with high standard curve PCR efficiency (95–105%) were accepted, and each sample was measured in triplicate. After the growth curves plateaued (as measured by qRT-PCR), samples were then tested for infectivity titers by $TCID_{50}$ assay to determine the peak infectious titers. Sequencing of structural genes of viruses released into the medium was also performed from the day 12 aliquot.

Epitope mapping of mutant viruses

MAb reactivity with the E proteins of each mutant was performed by indirect fluorescent antibody (IFA) assay (Gubler, 1987) using acetone-fixed virus-infected C6/36 cells. A dilution series of the following DENV2 MAbs (epitopes) was used to determine reactivity end-points: DI, 1B4C-2 (C1); DII, 4G2 (A1), 6B6C-1 (*A1*), and 2H3 (*A4*); DIII, 3H5 (*B1*), 9A3D-8 (*B2*), and 1A1D-2 (*B4*); and 2H2 (prM) (Roehrig et al., 1998). The MAb reactivity with each mutant virus was compared to that with 30P-NBX parental virus, and a four-fold or greater change in endpoint was considered significant.

E protein glycosylation. The glycosylation profiles of 30P-NBX and the mutant DENV KKK305/307/310EEE, G104S, and KK291/295EV were determined using previously published procedures for endoglycosidase H (endoH) and PNGase F deglycosylation (Bryant et al., 2007; Calvert et al., 2012). One modification in this protocol was made - using DENV EDII-reactive MAb 4G2 in the antibody affinity matrix to concentrate virus prior to glycosidase treatment.

Fusion-from-within (FFWI) assay

FFWI of virus-infected C6/36 cells was assayed as previously described (Butrapet et al., 2011; Huang et al., 2010). Percent cell fusion induced by mutants versus 30PA-NBX parental virus was calculated.

Virus attachment and growth measured by real time qRT-PCR

Generally, viral attachment and growth assays were performed by first allowing virus to attach at specific MOIs to Vero cells in 6-well plates at 4C for 1 h, pH 7.4. For growth and RNA synthesis analyses, after attachment and removal of unbound virus by rinsing with ice cold PBS, maintenance medium was added, and the plates were kept at 37C for 72 h. At 4 h post-attachment a sample of medium was removed to determine residual virus. At 72 h p.i. a second sample of medium was removed to determine the level of viral growth. At 72 h, total RNA was extracted from cells with Trizol, and the amount of DENV negative (−) sense vRNA was quantified as described below. Alternatively, viral attachment curves for Vero cells were generated by harvesting cells from a 6-well plate at 0, 5, 15, 30, 45, 60, and 90 min post-attachment at 4C, rinsing cells to remove unbound virus, and quantifying cell-associated vRNA using one-step qRT-PCR (as described above). Five μl of both types of extracted RNA were used to assess amounts of both (−) vRNA and vRNA, and each time point was repeated in triplicate.

Heparin inhibition. Heparin has been previously shown to inhibit DENV infection of human liver cells lines (Lin et al., 2002). In this study, we used HepG2 (human liver carcinoma) cell line for the heparin inhibition tests. Heparin inhibition was tested by pre-incubating a constant amount of virus (1×10^8 GE) with various concentrations (0, 0.1,1, 10, 100 and 1000 μg/ml) of soluble heparin (H-3149, Sigma). The mixtures were incubated in binding medium for 30 min at 4 °C, and then added to cells to determine binding as described above.

Quantitation of (−) vRNA

To detect RNA replication of mutants in Vero cells when a mutation was shown to be lethal, we conducted a 2-step RTqPCR procedure to quantitate DENV2 (−) vRNA using tagged primers as previously described (Huang et al., 2010) to minimize false amplification of cDNA during RT (Peyrefitte et al., 2003). Briefly, DENV2 primers and probes selected for the assay were from the 3′-non-coding genome region (Houng et al., 2001). A 19-nt Tag sequence (Peyrefitte et al., 2003) with no homology to DENV2 vRNA sequence was added to the 5′-end of the DENV2 primer, T-D2-10551, used for RT. For RT, template RNAs were denatured at 65 °C for 5 min in the presence of 1 μM T-D2-10551 primer and 0.6 mM dNTP mix. After RT, the amplified cDNA were quantified by qPCR using the iQ™ Supermix kit (BioRad) with 0.4 μM primers (Tag-primer containing only the 19-nt Tag and DENV2-specific primer CD2-10703), and 2 μM DENV2 probe (D2-10656P). In vitro transcribed (−) vRNA from a specifically-constructed plasmid containing the primer/probe-target DENV2 cDNA fragment was quantified and serially diluted to generate a standard curve for the 2-step RT-qPCR.

Virus growth in Raji cells expressing DC-SIGN

DC-SIGN transformed- and untransformed-Raji cells [a human B-cell lymphoma line (Epstein et al., 1966)] were gifts from Ted Pierson (NIAID, USA), and were used to assess viral growth in mammalian cells that express an alternative DENV receptor protein for which the virus binding motif is known. The expression of DC-SIGN was monitored by IFA with the DC-SIGN/DC-SIGNR reactive MAb, 1621 (R&D Systems, Minneapolis, MN). Parental 30P-NBX and mutant viruses (KKK305/307/309EEE, KK291/295EV, and G104S) were incubated with 1×10^6 cells of either type for 1 h at 4C, at various MOI. After absorption, nonattached virus was removed by rinsing in PBS. Virus-infected cells were then incubated for 3 days, and virus growth was measured by either detecting the expression of cell-associated *E* protein by IFA using a mouse hyperimmune ascitic fluid to DENV2, or qRT-PCR for progeny vRNA (see above). The mutants were evaluated in the same manner.

Statistical evaluation

Most results are reported as mean ± standard deviation from 3 or 4 separate experiments. Student's *t* test was used to test for significance, and results that had *p* values < 0.05 were considered significant.

Acknowledgments

We thank Ms. Mellisa Bushey, Ms. Kelley Moss, and Mr. Shawn Silengo for their technical assistance in various experiments, and Ted Pierson for the Raji cells. This study was supported by the Centers for Disease Control and Prevention, and a grant from the Pediatric Dengue Vaccine Initiative (PDVI TR-159A).

References

Boonnak, K., Slike, B.M., Burgess, T.H., Mason, R.M., Wu, S.J., Sun, P., Porter, K., Rudiman, I.F., Yuwono, D., Puthavathana, P., Marovich, M.A., 2008. Role of dendritic cells in antibody-dependent enhancement of dengue virus infection. J. Virol. 82, 3939–3951.

Bryant, J.E., Calvert, A.E., Mesesan, K., Crabtree, M.B., Volpe, K.E., Silengo, S., Kinney, R.M., Huang, C.Y., Miller, B.R., Roehrig, J.T., 2007. Glycosylation of the dengue 2 virus E protein at N67 is critical for virus growth in vitro but not for growth in intrathoracically inoculated Aedes aegypti mosquitoes. Virology 366, 415–423.

Butrapet, S., Childers, T., Moss, K.J., Erb, S.M., Luy, B.E., Calvert, A.E., Blair, C.D., Roehrig, J.T., Huang, C.Y., 2011. Amino acid changes within the E protein hinge region that affect dengue virus type 2 infectivity and fusion. Virology 413, 118–127.

Calvert, A.E., Huang, C.Y., Blair, C.D., Roehrig, J.T., 2012. Mutations in the West Nile prM protein affect VLP and virion secretion in vitro. Virology 433, 35–44.

Chen, Y., Maguire, T., Hileman, R.E., Fromm, J.R., Esko, J.D., Linhardt, R.J., Marks, R.M., 1997. Dengue virus infectivity depends on envelope protein binding to target cell heparan sulfate. Nat. Med. 3, 866–871.

Crill, W.D., Roehrig, J.T., 2001. Monoclonal antibodies that bind to domain III of dengue virus E glycoprotein are the most efficient blockers of virus adsorption to Vero cells. J. Virol. 75, 7769–7773.

Davis, C.W., Mattei, L.M., Nguyen, H.Y., Ansarah-Sobrinho, C., Doms, R.W., Pierson, T.C., 2006a. The location of asparagine-linked glycans on West Nile virions controls their interactions with CD209 (DC-SIGN). J. Biol. Chem. 281, 37183–37194.

Davis, C.W., Nguyen, H.Y., Hanna, S.L., Sanchez, M.D., Doms, R.W., Pierson, T.C., 2006b. West Nile virus discriminates between DC-SIGN and DC-SIGNR for cellular attachment and infection. J. Virol. 80, 1290–1301.

Diamond, M.S., Pierson, T.C., Fremont, D.H., 2008. The structural immunology of antibody protection against West Nile virus. Immunol. Rev. 225, 212–225.

Epstein, M.A., Achong, B.G., Barr, Y.M., Zajac, B., Henle, G., Henle, W., 1966. Morphological and virological investigations on cultured Burkitt tumor lymphoblasts (strain Raji). J. Nat. Cancer Inst. 37, 547–559.

Erb, S.M., Butrapet, S., Moss, K.J., Luy, B.E., Childers, T., Calvert, A.E., Silengo, S.J., Roehrig, J.T., Huang, C.Y., Blair, C.D., 2010. Domain-III FG loop of the dengue virus type 2 envelope protein is important for infection of mammalian cells and Aedes aegypti mosquitoes. Virology 406, 328–335.

Germi, R., Crance, J.M., Garin, D., Guimet, J., Lortat-Jacob, H., Ruigrok, R.W., Zarski, J.P., Drouet, E., 2002. Heparan sulfate-mediated binding of infectious dengue virus type 2 and yellow fever virus. Virology 292, 162–168.

Gromowski, G.D., Barrett, A.D., 2007. Characterization of an antigenic site that contains a dominant, type-specific neutralization determinant on the envelope protein domain III (ED3) of dengue 2 virus. Virology 366, 349–360.

Gubler, D.J., 1987. Application of serotype-specific monoclonal antibodies for the identification of dengue viruses. In: Yunker, C. (Ed.), Arboviruses in Arthropod Cells In Vitro. CRC Press, Boca Raton, FL, pp. 3–14.

Guirakhoo, F., Hunt, A.R., Lewis, J.G., Roehrig, J.T., 1993. Selection and partial characterization of dengue 2 virus mutants that induce fusion at elevated pH. Virology 194, 219–223.

Hacker, K., White, L., de Silva, A.M., 2009. N-linked glycans on dengue viruses grown in mammalian and insect cells. J. Gen. Virol. 90, 2097–2106.

Hilgard, P., Stockert, R., 2000. Heparan sulfate proteoglycans initiate dengue virus infection of hepatocytes. Hepatology 32, 1069–1077.

Houng, H.S., Chung-Ming Chen, R., Vaughn, D.W., Kanesa-thasan, N., 2001. Development of a fluorogenic RT-PCR system for quantitative identification of dengue virus serotypes 1-4 using conserved and serotype-specific 3′ noncoding sequences. J. Virol. Methods 95, 19–32.

Hsieh, P., Robbins, P.W., 1984. Regulation of asparagine-linked oligosaccharide processing. Oligosaccharide processing in Aedes albopictus mosquito cells. J. Biol. Chem. 259, 2375–2382.

Huang, C.Y., Butrapet, S., Moss, K.J., Childers, T., Erb, S.M., Calvert, A.E., Silengo, S.J., Kinney, R.M., Blair, C.D., Roehrig, J.T., 2010. The dengue virus type 2 envelope protein fusion peptide is essential for membrane fusion. Virology 396, 305–315.

Hung, J.J., Hsieh, M.T., Young, M.J., Kao, C.L., King, C.C., Chang, W., 2004. An external loop region of domain III of dengue virus type 2 envelope protein is involved in serotype-specific binding to mosquito but not mammalian cells. J. Virol. 78, 378–388.

Hung, S.L., Lee, P.L., Chen, H.W., Chen, L.K., Kao, C.L., King, C.C., 1999. Analysis of the steps involved in Dengue virus entry into host cells. Virology 257, 156–167.

Jennings, A.D., Gibson, C.A., Miller, B.R., Mathews, J.H., Mitchell, C.J., Roehrig, J.T., Wood, D.J., Taffs, F., Sil, B.K., Whitby, S.N., et al., 1994. Analysis of a yellow fever virus isolated from a fatal case of vaccine-associated human encephalitis. J. Infect. Dis. 169, 512–518.

Kuhn, R.J., Zhang, W., Rossmann, M.G., Pletnev, S.V., Corver, J., Lenches, E., Jones, C. T., Mukhopadhyay, S., Chipman, P.R., Strauss, E.G., Baker, T.S., Strauss, J.H., 2002. Structure of dengue virus: implications for flavivirus organization, maturation, and fusion. Cell 108, 717–725.

Lin, B., Parrish, C.R., Murray, J.M., Wright, P.J., 1994. Localization of a neutralizing epitope on the envelope protein of dengue virus type 2. Virology 202, 885–890.

Lin, Y.L., Lei, H.Y., Lin, Y.S., Yeh, T.M., Chen, S.H., Liu, H.S., 2002. Heparin inhibits dengue-2 virus infection of five human liver cell lines. Antiviral Res. 56, 93–96.

Lok, S.M., Kostyuchenko, V., Nybakken, G.E., Holdaway, H.A., Battisti, A.J., Sukupolvi-Petty, S., Sedlak, D., Fremont, D.H., Chipman, P.R., Roehrig, J.T., Diamond, M.S., Kuhn, R.J., Rossmann, M.G., 2008. Binding of a neutralizing antibody to dengue virus alters the arrangement of surface glycoproteins. Nat. Struct. Mol. Biol. 15, 312–317.

Marianneau, P., Megret, F., Olivier, R., Morens, D.M., Deubel, V., 1996. Dengue 1 virus binding to human hepatoma HepG2 and simian Vero cell surfaces differs. J. Gen. Virol. 77, 2547–2554.

Martinez-Barragan, J.J., del Angel, R.M., 2001. Identification of a putative coreceptor on Vero cells that participates in dengue 4 virus infection. J. Virol. 75, 7818–7827.

Modis, Y., Ogata, S., Clements, D., Harrison, S.C., 2003. A ligand-binding pocket in the dengue virus envelope glycoprotein. Proc. Nat. Acad. Sci. U.S.A. 100, 6986–6991.

Modis, Y., Ogata, S., Clements, D., Harrison, S.C., 2005. Variable surface epitopes in the crystal structure of dengue virus type 3 envelope glycoprotein. J. Virol. 79, 1223–1231.

Mukhopadhyay, S., Kim, B.S., Chipman, P.R., Rossmann, M.G., Kuhn, R.J., 2003. Structure of West Nile virus. Science 302, 248.

Mukhopadhyay, S., Kuhn, R.J., Rossmann, M.G., 2005. A structural perspective of the flavivirus life cycle. Nat. Rev. Microbiol. 3, 13–22.

Mukhopadhyay, S., Zhang, W., Gabler, S., Chipman, P.R., Strauss, E.G., Strauss, J.H., Baker, T.S., Kuhn, R.J., Rossmann, M.G., 2006. Mapping the structure and function of the E1 and E2 glycoproteins in alphaviruses. Structure 14, 63–73.

Munoz, M.L., Cisneros, A., Cruz, J., Das, P., Tovar, R., Ortega, A., 1998. Putative dengue virus receptors from mosquito cells. FEMS Microbiol. Lett. 168, 251–258.

Navarro-Sanchez, E., Altmeyer, R., Amara, A., Schwartz, O., Fieschi, F., Virelizier, J.L., Arenzana-Seisdedos, F., Despres, P., 2003. Dendritic-cell-specific ICAM3-grabbing non-integrin is essential for the productive infection of human dendritic cells by mosquito-cell-derived dengue viruses. EMBO Rep. 4, 723–728.

Nayak, V., Dessau, M., Kucera, K., Anthony, K., Ledizet, M., Modis, Y., 2009. Crystal structure of dengue virus type 1 envelope protein in the postfusion conformation and its implications for membrane fusion. J. Virol. 83, 4338–4344.

Peyrefitte, C.N., Couissinier-Paris, P., Mercier-Perennec, V., Bessaud, M., Martial, J., Kenane, N., Durand, J.P., Tolou, H.J., 2003. Genetic characterization of newly reintroduced dengue virus type 3 in Martinique (French West Indies). J. Clin. Microbiol. 41, 5195–5198.

Pletnev, S.V., Zhang, W., Mukhopadhyay, S., Fisher, B.R., Hernandez, R., Brown, D.T., Baker, T.S., Rossmann, M.G., Kuhn, R.J., 2001. Locations of carbohydrate sites on alphavirus glycoproteins show that E1 forms an icosahedral scaffold. Cell 105, 127–136.

Pokidysheva, E., Zhang, Y., Battisti, A.J., Bator-Kelly, C.M., Chipman, P.R., Xiao, C., Gregorio, G.G., Hendrickson, W.A., Kuhn, R.J., Rossmann, M.G., 2006. Cryo-EM reconstruction of dengue virus in complex with the carbohydrate recognition domain of DC-SIGN. Cell 124, 485–493.

Ramos-Castaneda, J., Imbert, J.L., Barron, B.L., Ramos, C., 1997. A 65-kDa trypsin-sensible membrane cell protein as a possible receptor for dengue virus in cultured neuroblastoma cells. J. Neurovirol. 3, 435–440.

Randolph, V.B., Winkler, G., Stollar, V., 1990. Acidotropic amines inhibit proteolytic processing of flavivirus prM protein. Virology 174, 450–458.

Rey, F.A., Heinz, F.X., Mandl, C., Kunz, C., Harrison, S.C., 1995. The envelope glycoprotein from tick-borne encephalitis virus at 2 A resolution. Nature 375, 291–298.

Roehrig, J.T., 2003. Antigenic structure of flavivirus proteins. Adv. Virus Res. 59, 141–175.

Roehrig, J.T., Bolin, R.A., Kelly, R.G., 1998. Monoclonal antibody mapping of the envelope glycoprotein of the dengue 2 virus, Jamaica. Virology 246, 317–328.

Salas-Benito, J.S., del Angel, R.M., 1997. Identification of two surface proteins from C6/36 cells that bind dengue type 4 virus. J. Virol. 71, 7246–7252.

Sukupolvi-Petty, S., Austin, S.K., Purtha, W.E., Oliphant, T., Nybakken, G.E., Schlesinger, J.J., Roehrig, J.T., Gromowski, G.D., Barrett, A.D., Fremont, D.H., Diamond, M.S., 2007. Type- and subcomplex-specific neutralizing antibodies against domain III of dengue virus type 2 envelope protein recognize adjacent epitopes. J. Virol. 81, 12816–12826.

Thaisomboonsuk, B.K., Clayson, E.T., Pantuwatana, S., Vaughn, D.W., Endy, T.P., 2005. Characterization of dengue-2 virus binding to surfaces of mammalian and insect cells. Am. J. Trop. Med. Hyg. 72, 375–383.

Thullier, P., Demangel, C., Bedouelle, H., Megret, F., Jouan, A., Deubel, V., Mazie, J.C., Lafaye, P., 2001. Mapping of a dengue virus neutralizing epitope critical for the

infectivity of all serotypes: insight into the neutralization mechanism. J. Gen. Virol. 82, 1885–1892.
Vogt, M.R., Moesker, B., Goudsmit, J., Jongeneelen, M., Austin, S.K., Oliphant, T., Nelson, S., Pierson, T.C., Wilschut, J., Throsby, M., Diamond, M.S., 2009. Human monoclonal antibodies against West Nile virus induced by natural infection neutralize at a postattachment step. J. Virol. 83, 6494–6507.
Volk, D.E., Gandham, S.H., May, F.J., Anderson, A., Barrett, A.D., Gorenstein, D.G., 2007. NMR assignments of the yellow fever virus envelope protein domain III. Biomol. NMR Assign. 1, 49–50.
Zhang, S.L., Tan, H.C., Hanson, B.J., Ooi, E.E., 2010. A simple method for Alexa Fluor dye labelling of dengue virus. J. Virol. Methods 167, 172–177.
Zhang, W., Mukhopadhyay, S., Pletnev, S.V., Baker, T.S., Kuhn, R.J., Rossmann, M.G., 2002. Placement of the structural proteins in Sindbis virus. J. Virol. 76, 11645–11658.
Zhang, Y., Corver, J., Chipman, P.R., Zhang, W., Pletnev, S.V., Sedlak, D., Baker, T.S., Strauss, J.H., Kuhn, R.J., Rossmann, M.G., 2003. Structures of immature flavivirus particles. EMBO J. 22, 2604–2613.